SHORT PAPER

J. Chem. Research (S),
2003, 105-107

Influence of perchloric acid on the crystalline phase of nanosized TiO_2 formed in reverse micelles

Ru-Bing Zhang and Ya-Fei Zhang

Research Institute of Micro/Nanometer Science and Technology, Shanghai Jiao Tong University, Shanghai 200030, P. R.China

Nanosized titania have been produced by the controlled hydrolysis of tetrabutyl titanate (TBT) in sodium bis(2-ethylhexyl)sulfosuccinate (SBS) reverse micelles. Nanoparticles could be produced at relatively high TBT concentrations. These nanoparticles aggregated into sols, with colloid sizes of 40–60 nm, eventually forming gelatinous precipitates. The effect of perchloric acid added during hydrolysis on the crystallinity of the titania nanopowders was investigated. The $HClO_4$ enhanced the phase transformations of the titania powders from amorphous to anatase as well as anatase to rutile. Different titania phases were produced, depending on the $[HClO_4]/[TBT]$ ratio. Thus $[HclO_4]/[TBT]=0.15$ yielded anatase at 80°C, while $[HClO_4]/[TBT]=0.20$ produced 100% rutile at 100°C.

Keywords: nanosized titania, perchloride acid, anatase, rutile,

Introduction

Titania powders find diverse applications[1-4] and they are typically made in the liquid or gas phase by the sulfate and chloride processes, respectively. However, it is known that the counteranions of the starting titanium salt remain in the product and deteriorate the purity of the powders.[5] To avoid counteranion contamination, titanium alkoxides can be used as the starting material for the titania particles. The aqueous phase of sodium bis(2-ethylhexyl)-sulfosuccinate reverse micelles, and water-in-oil microemulsions offer a unique environment in which to form metal oxide colloids, by the hydrolysis of metal alkoxide precursors in the nanosized droplets of water. Previous studies have shown that thermodynamically stable, monodisperse reverse micelles are formed in the $SBS/C_6H_{12}/H_2O$ system.

The transformation from amorphous to anatase has been reported in the literature to occur at temperatures from 400 to 600°C. Nevertheless, anatase-to-rutile phase transformation did not occur up to 800°C. [6]Bacsa [7]reported an improvement of the anatase-to-rutile phase transformation by peptising the hydrolysed precipitates with nitric acid (HNO_3) before heating treatment; however, l00% rutile phase was not obtained. Bischoff and Anderson found that acid catalysis of TiO_2 particles favoured the formation of rutile at room temperature, in comparison with the situation that occurred at higher temperatures.[8,9] Polycarboxylic acid was recently used as a catalysing agent, and the formation of nanoparticles of anatase was attributed to its chelation.[10] In the present paper, nano-TiO_2 sols were obtained under $HClO_4$ catalysis, even at room temperature. Electrophilicity of protons and nucleophilicity of perchloric ions are the proposed mechanisms for the formation of rutile and anatase phases at low temperature. The purpose of this work is to prepare nano-TiO_2 particles with high specific surface areas, as single phases of both rutile and anatase, or their mixtures; in addition, the influence of acid catalysis on the phase evolution of the TiO_2 will be investigated.

Experimental

Synthesis of nanosized TiO_2: $HClO_4$ and HNO_3 were used as hydrolysis catalysts. The molar ratio of catalyst/TBT was varied in the range of 0 to 0.2. Different amounts of the hydrolysis catalysts were mixed with a constant amount of water (molar ratio of water/TBT of 20). To moderate its high reactivity, ethylene diamine was added in a $SBS/C_6H_{12}/H_2O$ solution (molar ratio of TBT/ethylene diamine of 20) before reaction. For the hydrolysis experiments, the required volume of TBT (neat or a freshly prepared solution in C_6H_{12}) was added rapidly to a stirred $SBS/C_6H_{12}/H_2O$ solution containing various catalyst concentrations with a vigorous stirring for l h. On adding TBT to the mixed solution, a slurry containing white precipitate was formed. Clean liquid was removed through the slurry by filtering through a filter paper with openings less than or equal to 20–30 nm in diameter. The superfine precipitate was separated by centrifuging at l0,000 rpm for l0 min, dispersed in absolute acetone by ultrasonic wave, dried and then heated at various temperatures for 1 h in air. The microstructure and particle size were observed by transmission electron microscope (TEM). The crystalline phase was determined by the X-ray diffraction method (XRD). The crystallite sizes could be calculated from X-ray diffraction lines for anatase and rutile by Scherrer's equation. The specific surface area and pore structure were measured by the BET method.

Apparatus: The crystalline phases of samples were determined via X-ray diffraction (XRD) (Model D/MAX-C, Rigaku. Tokyo, Japan), using CuKα radiation. The specific surface area of powders was measured via nitrogen adsorption, using a surface area analyzer (ASAP-200, Micromeritics Instrument Group, USA). TEM(JEM-200CX, JEOL, Japan) was employed as roughly estimating particle size and shape. Raman measurements at room temperature were performed using the line at 488 cm^{-1} of an Ar laser (Equinox 55 model). Spectra were collected in a nearly back-scattering geometry on powdered samples in capillary tubes, using a double monochromator equipped with a photomultiplier and a photon counting system.

Results and discussion

Figure 1 illustrates the photos of TiO_2 nanoparticles, obtained by the procedure described earlier. The molar ratio of $[HClO_4]/[TBT]$ has a great influence on the grain size and crystallinity phase. As the molar ratio increases, the grain size also increases and phase transformation occurs. The powders catalysed in the molar ratio of $[HClO_4]/[TBT]$ of 0.15, were single phase of anatase (Fig.1(a)), which are spherical and of narrow size distributions. The grain boundaries among particles can be observed clearly, and the crystallite sizes determined from X-ray diffraction line for anatase were less than 30 nm. It was found that enhancement of $HClO_4$ concentration caused the growth of crystallites in full rutile phase. Their sizes and phases were dependent on the molar ratio of $[HClO_4]/[TBT]$: full rutile as $[HClO_4]/[TBT]=0.2$, shown in Fig. 1(b). The majority of rutile particles are rodlike, and the size distribution of particles is in the range 60–70 nm. The finding from our studies suggests that the growth of the primary particles is limited by the size of the interior micelles.

---

* To receive any correspondence. E-mail: zhang0911@sjtu.edu.cn

† This is a Short Paper, there is therefore no corresponding material in *J Chem. Research (M).*

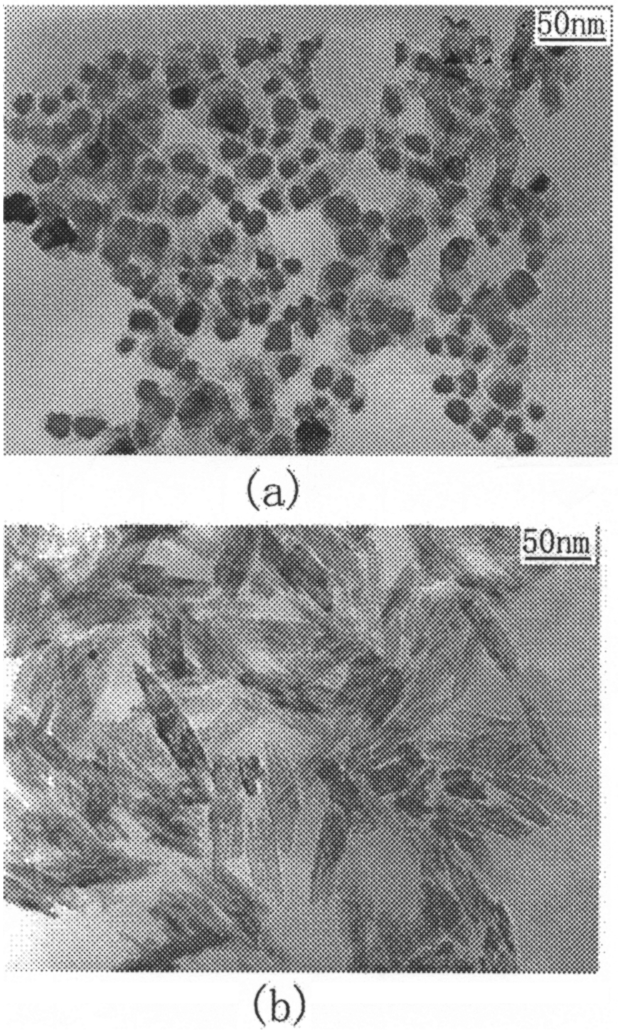

Fig.1 TEM images of TiO_2 nanoparticles: (a)anatase; (b)rutile.

Hence, primary particle formation may occur entirely in the aqueous interior of individual micelle. For rapid chemical reactions, it has been noted that micelles appear to act as separate, isolated entities where droplets exchange processes govern the overall reaction rate.[11] Since it is known that the reaction kinetics for the hydrolysis of TBT are very rapid, it is feasible that the formation of primary particles is an intramicellar process, and colloid/aggregate growth via micelle (forming large aggregates and ultimately precipitates) is the rate-limiting process.

The surface area values of as-prepared nano-TiO_2 are measured. Nonacidised sample derived from metatitanic acid has the lowest surface area of 28 m^2/g. Addition of $[HClO_4]/[TBT]$ to 0.15 increases the surface area to 92 m^2/g and further to 135 m^2/g for $[HClO_4]/[TBT]=0.20$. As is already known, the acidic catalysis is a result of complex sequence of hydrolysis and condensation reactions in which the gel is catalysed in the presence of perchloric acid. The condensation reactions lead to highly networked systems under $HClO_4$–catalysed conditions and are characterised by large specific surface areas and microporosities. Further, addition of $[HClO_4]$ enhances the strengthening of gel structure and thus increases resistance to drying stress, resulting in still higher surface area. The surface tension of $HClO_4$ during catalysis is preferentially less, and results in high specific surface area.

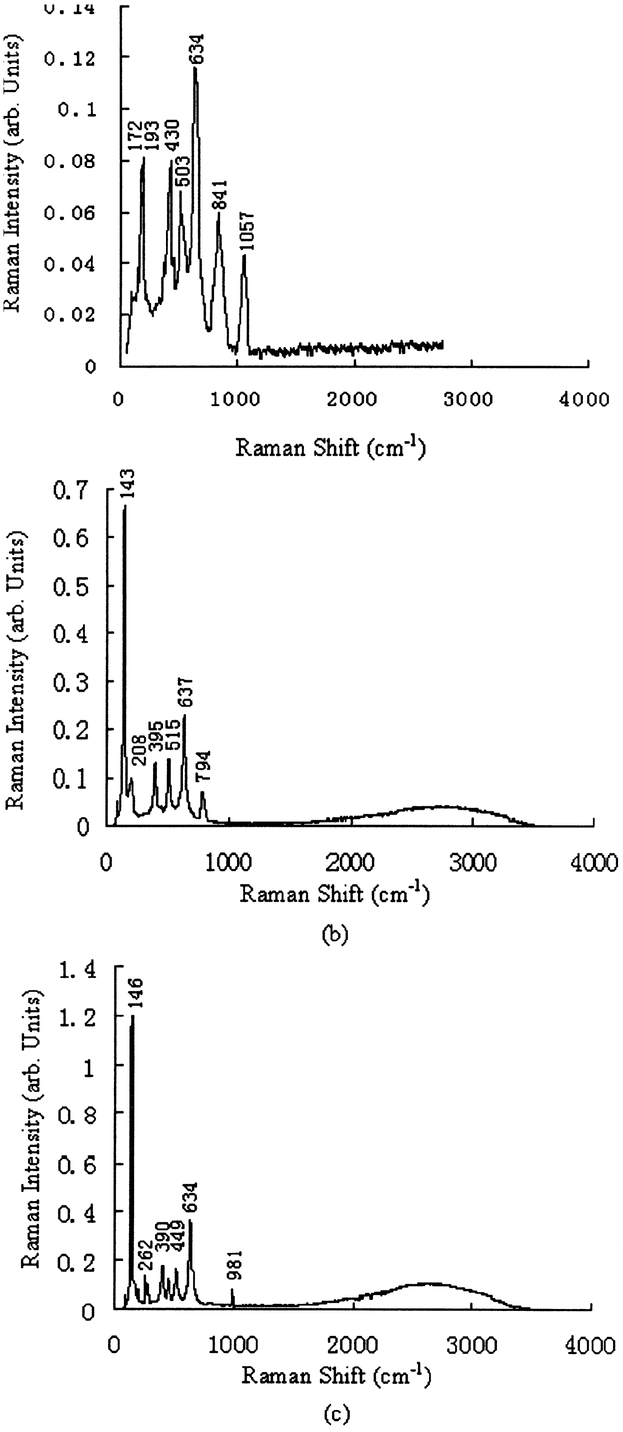

Fig.2 Raman spectra of nano-TiO_2 obtained using $HClO_4$ as catalyst :(a) amorphous; (b)anatase; (c)rutile.

In Fig. 2(a) the unacidised material spectrum shows three broad bands and two small peaks at 172, l93, 430,503,634, 841 and 1057 cm^{-1}, corresponding to TiO_2 in an amorphous state. The Raman spectra of nano-TiO_2 obtained using $HClO_4$ had features typical of the anatase and rutile phases,[12,13] confirmed by X-ray diffraction (XRD) analysis.[14] A progressive decrease in the widths of the Raman bands was observed at the higher $HClO_4$ concentrations. The 100% anatase phase was observed at the molar ratio of $[HClO_4]/[TBT]=0.15$ at 80°C, the spectrum is given in Fig. 2(b). The frequencies of the Raman bands observed are l43, 208, 395, 5l5, 637, and 794 cm^{-1}. The 143 cm^{-1} band is the strongest of all the

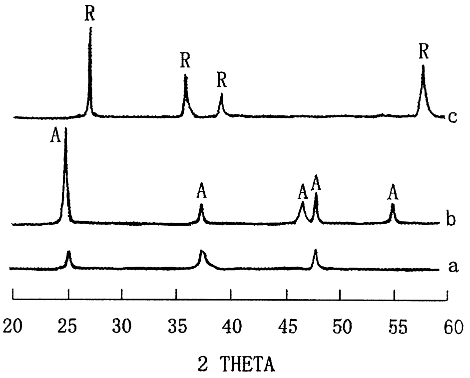

Fig.3. XRD patterns of nano-TiO_2 obtained using $HClO_4$ as catalyst: (a)anatase; (b)rutile.

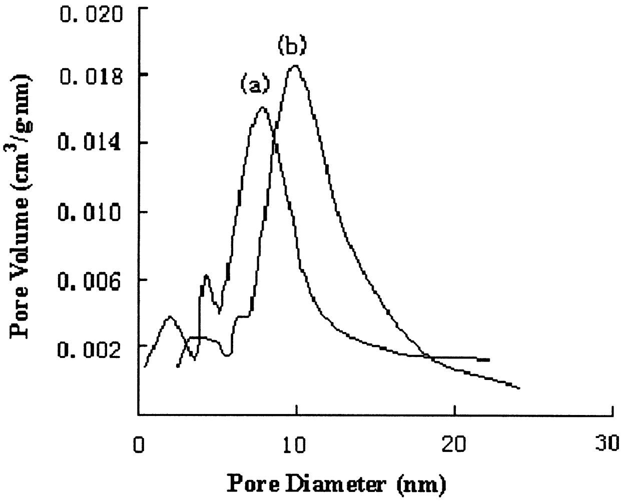

Fig.4. Pore distribution of the nanosized TiO_2. (a) $HclO_4$; (b)HNO_3.

observed bands in anatase. The anatase/rutile mixtures appear in the range of $[HClO_4]/[TBT]=0.15$ to 0.20 and pure rutile is obtained above $[HClO_4]/[TBT]=0.20$ at 100°C. Increasing the $[HClO_4]$ further leads to the transformation of anatase to rutile, and between these two spectra the relative intensities change. The changes could be interpreted as a precursor effect announcing the beginning of the anatase-rutile phase transition. The main effect in the transition is the progressive growth and narrowing of the 143 cm^{-1} peak. These results agree with XRD measurements.[15] Spectra presented in Figs 2(c) show the dominance of the rutile phase and the complete disappearance of the anatase phase. The rutile frequencies of the Raman bands observed at 100°C are 146, 262,390, 449, 634, and 981 cm $^{-1}$. A sharpening of the 146 cm^{-1} occurs, probably indicating the growth of microcrystallites. At this point it is important to observe that the difference between conditions used to obtain spectra 2(b) and 2(c) is the ratio of $[HClO_4]$ to [TBT], indicating that once the crystallisation process is initiated, it continues as a function of $HClO_4$ concentrations.

Acidification treatment has significant effects on the crystallographic phases that are formed within the particles. Figure 3 shows XRD patterns of acidised nano-TiO_2 powders. The nonacidized precipitates mainly were amorphous, especially for the sample that was obtained in the absence of $HClO_4$ or HNO_3 (not shown). For powder acidised by perchloric acid, pattern "a" in Fig. 3 exhibits very broad bands around 80°C, which correspond to the main anatase peaks and indicate a very low degree of crystallinity. Particles that have been peptised with a greater amount of $HClO_4$ ($[HClO_4]/[TBT]=0.20$) exhibit 100% rutile phase [Fig.3(b)]. Acification evidently promoted the crystallisation of both anatase and rutile phases. On the other hand, TiO_2 nanoparticles were obtained in the HNO_3 acidification process, in a manner similar to that which was used with $HclO_4$. However, in these samples, formation of the rutile phase is less favored. Anatase with a small amount of rutile was formed in the HNO_3-acidised samples that were treated at 350°C, whereas highly crystallised anatase phase without rutile was obtained at 300°C. Rutile with a high degree of crystallinity still was formed at 450°C. It is apparent that the transformation temperature of anatase to rutile is 200°C lower for $HclO_4$ than for the HNO_3–obtained powder. From the measurement of XRD and Raman spectroscopy, we concluded that with $HClO_4$, the molecular structure of the titania precursor resembled that of the crystalline anatase or rutile because the crystalline phase is more stable than the amorphous phase in low pH solutions.

Figure 4 shows the pore size distributions of the titania nanoparticles made in the presence of $HClO_4$ and HNO_3, respectively. The powders made at low $HClO_4$ concentration ($[HClO_4]/[TBT] = 0.15$) show bimodal pore size distributions consisting of fine intra-aggregated pores with a constant maximum pore diameter of 2–4 nm and larger interaggregated pores with pore diameters of 8 nm. A bimodal pore size distribution is due to the hard aggregates and two types of pores in the powders. One is fine intra-aggregated pores and the other is larger interaggregated pores. It is interesting to note that even though the amount of $HClO_4$ catalyst increases, the average pore size of the intra-aggregated pores shows a constant diameter of 8 nm. However, the powder prepared with excess $HClO_4$ concentration shows only intra-aggregated pores having an average diameter in the microporous region. The difference in the pore size distributions between powders prepared at low $[HClO_4]/[TBT]$ ratios and powders made with excess $HClO_4$ can be explained by the influence of the acidification step on the dispersion of primary particles in the sol. For the powder prepared under excess $HClO_4$ concentration, protons from $HClO_4$ are adsorbed on the surface of the primary particles. Assuming that all particles have the same surface charge, the particles are repelled and a stable sol results in a minimum degree of aggregation. On the other hand, the sol consisting of nano-TiO_2 prepared at low $HClO_4$ concentrations contains nonuniform, highly aggregated clusters of primary particles. The dried powders prepared using HNO_3 catalyst exhibit bimodal pore size distributions, consisting of fine intra-aggregated pores and larger interaggregated pores. All powders show constant average diameters of 6 and 10 nm for the intra-aggregated and interaggregated pores, respectively, regardless of the HNO_3 concentration. The pore volumes of the average diameters of the intra-aggregated pores decrease with increasing the HNO_3 concentration.

Conclusion

The crystallinity of nano-TiO_2 is dependent on the role of the specific reagent (perchloric acid). Acidification has an important role in determining the crystalline phases that are obtained. Rutile phases with high specific surface areas can be obtained by catalysing the sol-gel-derived TiO_2 precipitates with $HClO_4$ ($[HClO_4]/[TBT]=0.20$). Perchloric acid favours the formation of anatase and rutile, whereas the rutile phase is difficult to form when HNO_3 serves as the acidic catalyst.

Received 23 June 2002; accepted 23 September 2002
Paper 02/1435

References

1 E.A. Barringer and H.K. Bowen, *Langmuir*, (l985) **l**, 414
2 S. Vemury and S.E. Pratsinis, J. Am.Ceram. Soc., (1995) **78**, 2984.
3 G.P. Fotou, S.Vemury and S.E. Pratsinis, *Chem. Eng. Sci.*, (l994) **49**, 4939.
4 B. O'Regan and M. Graetzel, *Nature*, (l99l) **353**, 737.
5 H. Kondnami, Y. Takada, H. Yamagiwa, Y. Kera, M. Inoue and T. Inui, *J. Mater. Sci. Lett*., **15**, l97 (l996).
6 Y. Oguri, R.E. Riman and H.K. Bowen, *J. Mater. Sci*., (l988) **23**, 2897.
7 R.R. Bacsa and M. Gratzel, *J. Am. Ceram*. Soc., (l996) **79**, 2185.
8 B.L. Bischoff and M. Anderson, *Chem. Mater*., (l995) **7** 1772.
9 K.-N.P. Kumar, J. Kumar and K. Keizer, *J Am. Ceram. Soc*., (1994) **77** l396.
10 T.Y. Zeng, Y. Qiu, L. Chen and X.. Song, *Mater. Chem. Phys*., (l998) **56** l63.
11 P.D.Fletcher and B.H.Robinson, *Phys.Chem*. (1981) **85**,863
12 P.P. Lottici, D. Bersani, M. Braghini and A. Montenero, *J. Mater. Sci*. (l993) **28** l77.
13 U. Balachandran and N.G. Eror, *J. Solid State Chem*. (1982) **42** 276.
14 Bohkimi, A. Morales, O. Novaro, T. Lopez, E. Sanchez and R. Gomez. *J. Mater. Res*. (l995) **l0** 2788.
15 T. Lopez, E. Sanchez, P. Bosch, Y. Meas and R. Gomez, *Mater. Chem. Phys.* (l992) **32** l4l.